

# Experimental Investigations of the Spherical Taylor-Couette Flow

M. Mahloul<sup>1†</sup>, A. Mahamdia<sup>1</sup> and M. Kristiawan<sup>2</sup>

<sup>1</sup> Faculty of Physics, University of Sciences and Technology "Houari Boumediene",  
 Algiers, 16111, , Algeria

<sup>2</sup> INRA, UR 1268 Biopolymers Interactions and Assemblies, Nantes, 44316, France

†Corresponding Author Email: [mmahloul@yahoo.fr](mailto:mmahloul@yahoo.fr)

(Received October 20, 2015; accepted December 10, 2015)

## ABSTRACT

Transition to turbulence of a viscous incompressible fluid flow between two concentric spheres with the inner one rotating and the outer stationary was investigated experimentally. The flow modes were studied using the flow visualization and electrochemical technique. Different flow states were obtained for the gap/radius ratio 0.107 in function of the Taylor number in the interval (22 - 1500) and aspect ratio (17 - 21). Observed states were classified into: Taylor Vortex Flow (TVF), Spiral Mode (SM), Spiral Mode & Wavy Mode (SM+WM), Spiral Wavy Mode (SWM), Wavy Mode (WM) and Chaos. The variations of the flow patterns were reflected by the wall velocity gradient, its fluctuation and spectral analysis. Fast Fourier transform applied on the time series of the wall velocity gradient allowed for the analysis and identification of the fundamental frequencies and their evolutions associated with each flow state.

**Keywords:** Spherical taylor-couette; Mode; Instability; Visualization; Electrochemical method.

## NOMENCLATURE

$d$	gap width= $(R_2-R_1)$	$Tc_4$	critical value of Spiral Wavy Mode
$H$	height of liquid	$Tc_5$	critical value of azimuthal waves
$R_1$	radius of inner sphere	$Tc_6$	the near-turbulence regime
$R_2$	radius of outer sphere	$Tc_7$	onset of chaos
$S$	wall velocity gradient	$Tc_8$	developed turbulence
$s'$	fluctuation intensity of $S$	$\beta$	gap / radius ratio = $d / R_1$
$v$	azimuthal velocity	$\Gamma$	aspect ratio = $H/d$
<i>Subscripts</i>		$\mu$	dynamic viscosity
$Tc_1$	critical value of start-up of Taylor vortices	$\theta$	angle measured from the sphere axis
$Tc_2$	critical value of Spiral Mode	$\tau$	local friction coefficient
$Tc_3$	onset of Spiral Mode and Wavy Mode	$\Omega$	angular frequency

## 1. INTRODUCTION

In the present work the behavior of the spherical Couette flow in a closed system with the gap/radius ratio  $\beta = d / R_1 = 0.107$  is examined experimentally for the aspect ratio  $\Gamma = H / d$  in the range (17-21) and over a wide range of Taylor number (22-150) defined as

$$Ta = R_1 \Omega d / \nu \sqrt{d / R_1} \quad (1)$$

Studies on the spherical Couette flow are of basic importance particularly for the understanding of symmetry-breaking bifurcations during the

transition to turbulence.

Experimental investigations using different visualization techniques of the stability behaviour of the flow in spherical gap can be found in the works of Khlebutin (1968), Sawatzki and Zierep (1970), Munson and Menguturk (1975), Yavorskaya *et al.* (1975), Nakabayashi (1978) and Wimmer (1981).

Wimmer (1981, 1988) showed that the flow modes depend not only on  $Ta$  and  $\beta$  but also on acceleration history of the inner sphere.

Menguturk and Munson (1975) studied the torque

as a function of flow regimes in large gap  $\beta=1.27$ . Their results are in a good agreement with experiments and perturbation theory for narrow gap values. The torque was also measured by Nakabayashi (1978) over a range of Reynolds number and gap ratio. He established empirical formulas for the coefficient of frictional moment for each flow regime.

Egbers and Rath (1995) confirmed experimentally the existence of Taylor vortices and different instabilities during the laminar-turbulent transition. However, they did not obtain Taylor vortices in wider gaps ( $0.33 \leq \beta \leq 0.50$ ).

Nakabayashi *et al.* (2000, 2005) found a relaminarization effect in the laminar-turbulent transition in  $0.13 < \beta < 0.17$ .

On the other hand, several numerical investigations were carried out for small gaps. The numerical simulations for a larger gap are rather difficult. Yuan (2012) investigated numerically the flow of wavy and spiral Taylor-Görtler vortices in spherical gaps for  $\beta=0.14$  and  $0.18$  imposing different wave number and perturbations. Furthermore, the flow between concentric and eccentric rotating spheres was investigated by means of finite element method by Bar-Yoseph *et al.* (1990, 1992). Using finite difference method, Bühler (1990) demonstrated the existence of flow asymmetry with respect to the equator.

The bifurcation behaviour and asymmetric modes in Newtonian fluids were examined by Mamun and Tuckerman (1995). They presented bifurcation diagrams with torque characteristics.

Possible flow modes were investigated by Yang (1996) who used in his model axisymmetric boundary conditions.

Feudel *et al.* (2013) studied the multistability and particularly the route to chaos, consecutive bifurcations and the spatiotemporal features in rotating spherical shell.

Experimental study of the spherical Taylor-Couette flow, using electrochemical technique, is the original motivation of the present work. The ultimate goal is the evolution of the different modes during the transition from laminar flow to turbulence. The results obtained allow us to examine the evolutions of the velocity gradient ( $S$ ), the local friction coefficient ( $\tau$ ) and the fluctuating rate  $s'/S$  versus the Taylor number for various values of the aspect ratio  $\Gamma$ . The hydrodynamic instabilities for different regimes are investigated by spectral analysis of time series recorded for the different observed flows.

## 2. EXPERIMENTAL CONDITIONS

The experimental setup consists of two concentric spheres made of transparent Plexiglas. The outer sphere with radius  $R_2 = 54.9$  mm is at rest, while the inner one with radius  $R_1 = 49.6$  mm rotates about the common vertical axes with an angular velocity  $\Omega_1$  (Fig. 1).

Direct current motor drives the inner sphere at a speed varying between  $0.01$  and  $3.01$  rev/s. The temperature is controlled and measured using an electronic gauge with accuracy better than  $0.01^\circ\text{C}$ .

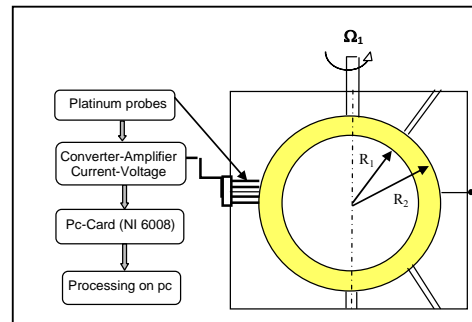


Fig. 1. Experimental setup.

The working fluid is an aqueous solution of potassium ferri-ferrocyanide with equimolar concentration of  $2 \text{ mol/m}^3$ . The concentration of the supporting electrolyte potassium sulfate is  $300 \text{ mol/m}^3$ . For the purpose of flow visualization, 2% of Kalliroscope AQ 1000 are added to the solution.

A total of ten platinum micro-probes of  $0.5$  mm diameter are used in the present study. The anode (counter electrode) is a platinum sheet with dimensions  $50 \times 20$  mm attached to the bottom of the inner wall of the outer sphere (Fig. 2).

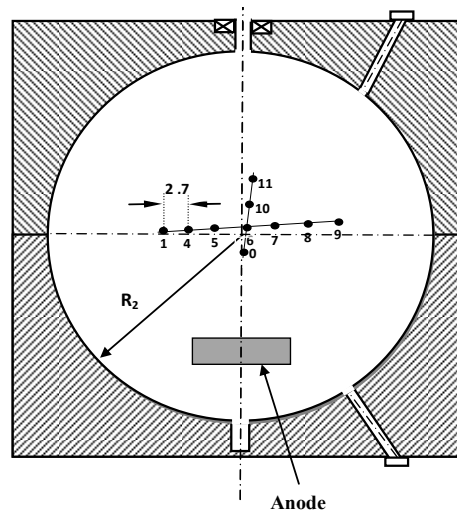


Fig. 2. The probes location in the outer sphere.

The electrochemical method was already used in the cylindrical Taylor-Couette apparatus by Cognet (1971), Mahamdia (2005), Sobolik *et al.* (2011) and conical Taylor-Couette set-up by Noui *et al.* (2004). This is for the first time, when this technique is used for the spherical Couette flow.

This method is based on the measurement of the limiting diffusion current  $I$ , which is associated with the mass transfer coefficient on the working electrode – the probe (cathode). By means of

imposing a potential, which is different from the equilibrium potential, an oxidation-reduction reaction occurs on the electrodes which causes ion displacement in the solution. The mass transfer is composed of convection, diffusion and migration of active ions between anode and cathode due to the redox reaction. Supporting electrolyte suppresses the migration. The velocity gradient on the probe can be deduced from the limiting diffusion current which depends only on the convection and diffusion.

In the quasi-steady boundary layer approximation (Leveque, 1928), the velocity gradient  $S$  on the probe is related to the limiting diffusion current by the equation:

$$S = 0.0996 \frac{I^3}{(nFc)^3 D^2 R^5} \quad (2)$$

where  $I$  is the electric current,  $n$  the number of electrons implied in the redox reaction,  $F$  the Faraday constant,  $R$  the electrode radius,  $D$  the diffusion coefficient and  $c$  the concentration of active ions in the bulk.

The analysis of the measured current allowed us to study temporal variations of wall velocity gradient. The signals were treated in two stages: firstly the mean component was calculated by averaging the current recorded during 5 minute at a probe, and then the current was high pass filtered to remove the mean component and to obtain the fluctuations intensity. The power spectra obtained by means of a PC-card (NI 6008) connected to a computer and a Fast Fourier Transform (FFT) algorithm written in MATLAB permitted the determination of the characteristic frequencies related to the nature of every observed flow.

### 3. RESULTS AND DISCUSSION

The results concern experimental study of the flow in the gap between two concentric spheres, where the inner sphere rotates and the outer one is at rest. The results are presented in terms of Taylor number and aspect ratio (Fig. 3).

The critical Taylor number,  $T_c$ , at which the transition occurs, identifies the different flow regimes. The flow state near the equator is rather similar to the flow between concentric rotating cylinders.

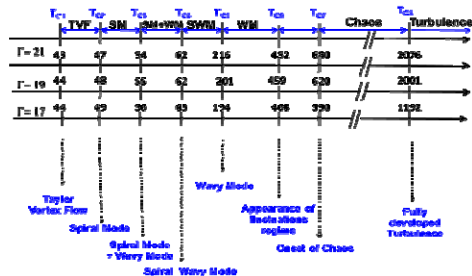


Fig. 3. Diagram of the appearance of instability modes for different aspect ratios  $\Gamma$ : TVF, SM, SM+WM, WM, Chaos and Turbulence.

The rotation rate of the inner sphere was quasi statically increased from rest. For Taylor numbers under  $T_{c1} = 43$ , the flow is stable and no instabilities are observed. As  $Ta$  is close to 0, the flow is illustrated by streamlines in the form of concentric circles with circumferential velocity component (Bühler, 1990)

$$v(r, \theta) = \frac{\Omega R_1^3 (r^3 - R_2^3)}{r^2 (R_1^3 - R_2^3)} \sin \theta \quad (3)$$

The meridian and radial velocity components are zero. This regime is due to the balance between the inertial forces and viscous forces. The basic laminar flow in this system is a steady axisymmetric and equatorially symmetric three-dimensional flow.

The Taylor vortex flow (TVF) is the first instability mode in the spherical Taylor-Couette flow. This mode is composed of four cells, a symmetrical configuration of a pair of toroidal vortices on each side of the equator (Fig. 4a). In the remaining part of the spherical gap, the streamlines have a spiral shape but are not visible because of the slow fluid motion. The thickness of the gap has stabilizing effect on the Taylor vortex flow. The thinner the fluid layer between the spheres the more stable the flow:  $T_{c1} = 41.3 (1 + \beta)$  (Yavorskaya, 1980). Using this formula for our case of  $\beta = 0.107$ , the critical Taylor number would have a value of 45.7. We found a value of 43.5 for  $\Gamma = 21$ . This value slightly increases with decreasing aspect ratio. Our critical Taylor number of the first instability mode for the gap ratio  $\beta = 0.107$  is compared with previous experimental and numerical works in Table 1.

Table 1 Comparison of critical Taylor number  $T_{c1}$  of the Taylor vortex flow.  $\beta = 0.107$ ,  $\Gamma = 21$ .

Experimental	
Present work	43.50
Wimmer (1976)	42.99
Yavorskaya (1980)	45.70
Khlebutin (1968)	49.00
Numerical	
Walton (1978)	43.03

The second instability, i.e. spiral mode (SM), corresponds to a regime that occurred at the Taylor number  $T_{c2} = 47$ . It is composed of four Taylor cells at the equator and additional spirals in the rest of the spherical gap; see Fig. 4b. The spirals have an inclination between  $2^\circ$  and  $10^\circ$  with respect to the equator and move from the equator towards the poles as reported by Wimmer (1976) and Nakabayashi (1983).

The regime composed of four wavy Taylor cells in the vicinity of equator and spirals which stretch out in each hemisphere, the spiral mode & wavy mode, occurs at a critical value  $T_{c3} = 53$  (Fig. 4c). The amplitude of the waves is small at the equator and increases with increasing distance from the equator.

Beyond a critical value  $T_{c4} = 62$ , corresponding to the onset of spiral way mode (SWM), the flow takes

a form of wavy Taylor vortices at the equator and wavy spirals in the rest (Fig. 4d). The spirals propagated from the equator to the two poles at increasing velocity.

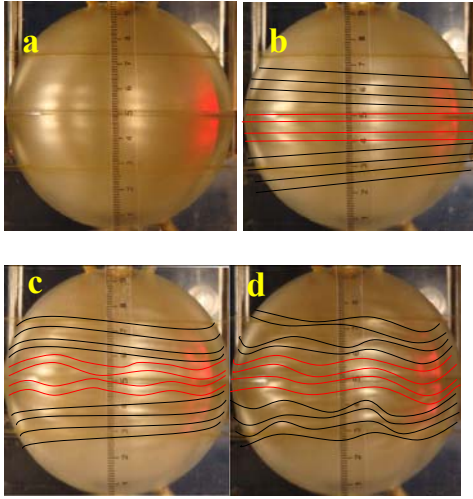


**Fig. 4. Visualization of:** (a) Taylor Vortex Flow,  $Tc_1=43$ , (b) Spirals Mode,  $Tc_2=47$ . (c) Spiral Mode and Wavy Mode,  $Tc_3=54$ . (d) Spiral Wavy Mode,  $Tc_4=62$ .

The fifth instability is the wavy mode (WM). It is detected at a critical Taylor number  $Tc_5=216$ . This mode is observed in the entire gap (Fig. 5a) and seems to be similar to the flow pattern in cylindrical and conical Couette flow. The effect of the acceleration is important for the onset of the wavy mode.

With increasing Taylor number, the flow pattern becomes progressively chaotic. The near-turbulent regime is evident through the presence of fluctuations at the poles at the Taylor number  $Tc_6=452$ . These fluctuations propagate gradually into the equatorial part. While increasing the rotation rate, the azimuthal waves gradually attenuate. Beyond the critical value  $Tc_7=680$  the Taylor cells at the equator are filled by turbulent flow. The flow in the rest of the gap is chaotic (Fig. 5b). Finally, at a critical value  $Tc_8=2076$ , the regime of fully developed turbulence starts through the whole gap.

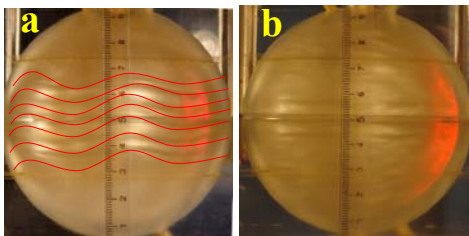


**Fig. 5. Visual observation of:** (a) Wavy Mode,  $Tc_5=216$  and Chaos,  $Tc_7=680$ .

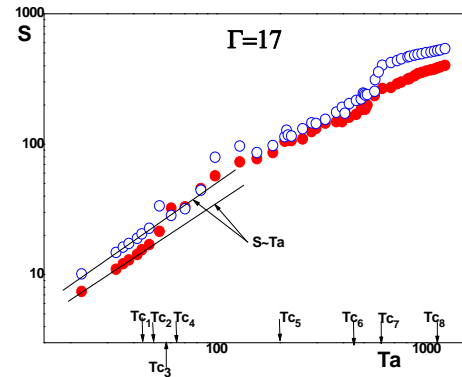
In the next, we present the evolutions of the

velocity gradient  $S$ , the local friction coefficient  $\tau$  and the fluctuating rate  $s'/S$  as a function of the Taylor number for different values of the aspect ratio  $\Gamma$ .

When  $Ta$  is close to zero, the velocity gradient at the outer sphere is expressed by the derivative of Eq.3 with respect to  $r$

$$S = \left. \frac{\partial v}{\partial r} \right|_{r=R_2} = \frac{3\Omega R_1^3}{R_2^3 - R_1^3} \sin \theta \quad (4)$$

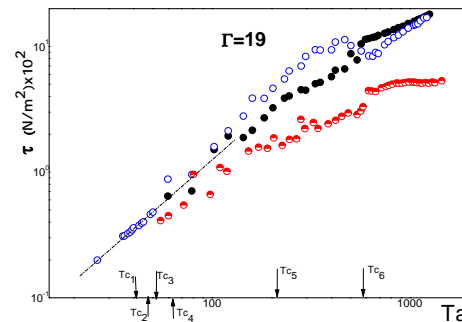
The wall velocity gradients measured by two probes, show an increase with Taylor number (Fig. 6).



**Fig. 6. Evolution of the mean wall velocity gradient versus Taylor number. Open circles stand for probe 5 and solid circles for probe 7.**

The values of  $S$  for  $Ta < Tc_3$  are independent of time, thus indicating that the flow is stationary. In the laminar basic flow, the measured velocity gradient is proportional to the Taylor number ( $S \sim Ta$ ). It should be noted that the uncertainty of wall shear rate measurements is 6%.

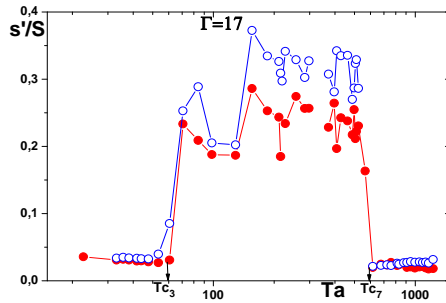
The determination of  $S$  by the electrochemical method enables access to local friction coefficient  $\tau = \mu S$  (Fig. 7).



**Fig. 7. Evolution of the local friction coefficient versus Taylor number. Open circles stand for probe 5, half solid circles for probe 10 and solid circles for probe 7**

The intensity of the velocity fluctuations,  $s'/S$ ,

sharply increases at  $Tc_3$  when the spiral Taylor-Görtler vortices start up, see Fig. 8. With increasing Taylor number, the fluctuations remain almost constant until  $Tc_7=680$ , when the intensity suddenly attenuates and tends to zero. This trend, shown in Figs 8 and 9, is known as relaminarization. Similar behavior was observed by Nakabayachi *et al.* (2000, 2005) using LDV method.



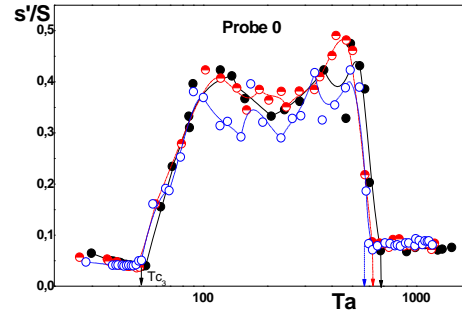
**Fig. 8. Evolution of non-dimensional fluctuations intensity,  $s'/S$ , versus Taylor number for  $\Gamma=17$ . Open circles stand for probe 4 and solid circles for probe 11.**

Figure 9 shows the influence of the aspect ratio  $\Gamma$  on the appearance of chaos. When the aspect ratio increases, the start of chaos is postponed to higher Taylor number.

Results of spectral analysis are shown in Fig.10. The fundamental frequency ( $f_0 = 0.115$  Hz), with its harmonics and subharmonics, is apparent in the power spectrum of wavy Taylor vortices at  $Ta=202$ . This frequency is linked to the rotation rate of the sphere. The ratio of  $f_0$  over the rotation rate of the inner sphere  $N = \Omega/2\pi$  has a value of  $f_0/N \approx 0.33$ . This value agrees well with the results obtained in the cylindrical *Taylor-Couette* flow by Coles (1965) and Bouabdallah (1980) and in the flow between conical cylinders (Wimmer, 1995). The peak of  $4 \times f_0$  is higher than those of the other entire harmonics, which means that there are four azimuthal waves superposed on the Taylor vortices. This is also consistent with the calculation of Chossat and Ioos (1994) for the bifurcation of spirals in Taylor-Couette systems. They found the flow quasi-periodic with two independent frequencies, one linked to the basic spirals and the other representing the wavy motion of the spirals. The azimuthal waves on Taylor vortices at  $Ta = 603$  are almost attenuated. There is the fundamental frequency  $f_0$  and its harmonics in Fig.10. The angular frequency at  $Ta=603$  is about three times higher than at  $Ta=202$ , but the ratio of the fundamental frequencies is only 1.7. This means that the vortices rotate with a relative velocity lower than 0.33. Such result is not surprising since the value 0.33 was found close to the bifurcation.

The power spectrum of chaos is flat without any dominant frequency (Fig. 10,  $Ta=680$ ).

In the present study, we used the electrochemical method for measuring  $S$ ,  $\tau$ ,  $s'/S$  and observed different modes of instability.



**Fig. 9. Evolution of non-dimensional fluctuations intensity,  $s'/S$ , a function Taylor number for different aspect ratio  $\Gamma$ . Open circles for  $\Gamma=18$ , half solid circles for  $\Gamma=19$  and solid circles stand for  $\Gamma=21$ .**

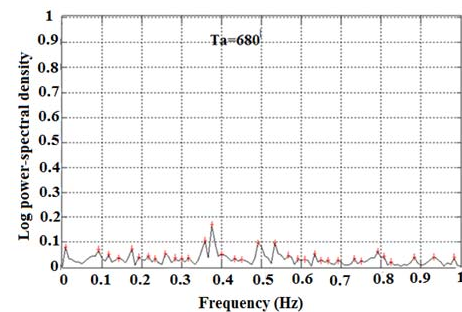
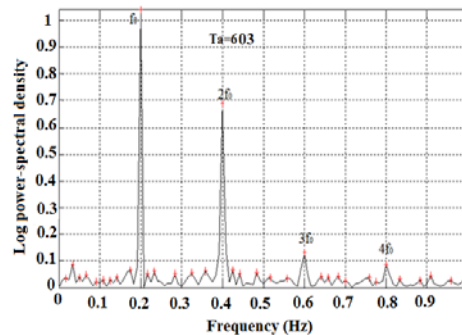
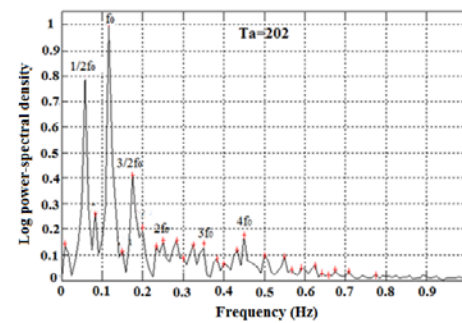


**Fig. 10. Power spectral density evolution versus the frequency measured with the electrode 0 at  $\Gamma=21$ . Spiral wavy mode at  $Ta = 202$ , azimuthal waves at  $Ta = 603$  and chaos at  $Ta = 680$ .**

#### 4. CONCLUDING REMARKS

As the Taylor number was increased; the Taylor

vortices flow was replaced by spiral mode, spiral mode and wavy mode and spiral wavy mode. For higher Taylor numbers, the wavy mode disappeared due to the setting of chaos mode, and at last the flow degenerated to a fully developed turbulence.

The examination of the results and particularly the variation of the mean wall velocity gradient with the Taylor number helped us to highlight the different flow regimes when gradually increasing the velocity of the inner sphere. The evolution of the wall velocity gradient with  $Ta$  was linear until  $Ta=47$ , then the increase was more pronounced up to  $Ta=227$ .

The relaminarization phenomenon was observed. Important increase of the wall velocity gradient fluctuations measured close to the equator started at  $Ta=54$ . The high fluctuations lasted until  $Ta=680$ , where a sharp decrease was observed as the consequence of turbulent flow.

Azimuthal waves manifested themselves by peak in power spectra. The chaotic and turbulent regimes resembled white noise.

The present investigation revealed the routes towards chaos in spherical Couette flow. Nevertheless the observed phenomena need further experimental study.

## REFERENCES

- Bar-Yoseph, P. A. Solan., R. Hillen., and K. G., Roesner (1990). Taylor vortex flow between eccentric coaxial rotating spheres. *Physics of Fluids* 2, 1564-1573.
- Bar-Yoseph, P., K. G. Roesner, and A. Solan (1992). Vortex breakdown in the polar region between rotating spheres. *Physics of Fluids* 4, 1677-1686.
- Bouabdallah, A. (1980). *Instabilités et turbulence dans l'écoulement de Taylor-Couette*. Ph. D. Thesis, Université de Nantes, France.
- Bühler, K., and J. Zierp (1985). New secondary instabilities for high Re-number flow between two rotating spheres, in: Kozolov, V.V. (ed.): *Laminar-Turbulent Transition. IUTAM Symp, Novosibirsk/USSR, Springer*, 677-685.
- Bühler, K. (1990). Symmetric and asymmetric Taylor vortex flow in spherical gaps. *Acta Mechanica* 81, 3-38.
- Cognet, G. (1971). Utilisation de la polarographie pour l'étude de l'écoulement de Couette. *Journal de Mécanique* 10, 65-90.
- Chossat, P., and G. loos (1994). *The Taylor-Couette problem*. Springer, Berlin.
- Coles, D. (1965). Transition in circular Couette flow, *Journal of Fluid Mechanics* 21, 385-425.
- Egbers C, and H. J., Rath (1995). The existence of Taylor vortices and wide-gap instabilities in spherical Couette flow. *Acta Mechanica* 111, 125-140.
- Feudel, F., N. Seehafer, L. S. Tuckerman, and M. Gellert (2013). Multistability in rotating spherical. shell convection. *Physical Review E* 87, 023021.
- Khlebubin, G. N. (1968). Stability of fluid motion between a rotating and a stationary concentric sphere. *Journal Fluid Dynamics* 3, 31-32.
- Leveque, M. A. (1928). Les lois de la transmission de chaleur par convection. *Ann Mines* 13, 201-239.
- Mahamdia, A., A. Bouabdallah, and S. Skali (2005). Ecoulement de Taylor-Couette en géométrie finie et à surface libre. *The Canadian Journal of Chemical Engineering* 83, 652-657.
- Mamun, C. K, and L. S. Tuckerman (1995). Asymmetry and Hopf bifurcation in spherical Couette flow. *Physics of Fluids* 7, 80-91.
- Menguturk, M, and B. R. Munson (1975). Experimental results for low Reynolds number flow between eccentric rotating spheres. *Physics of Fluids* 18(2), 128-130.
- Munson, B. R, and M. Menguturk (1975). Viscous incompressible flow between concentric rotating spheres. Part 3, Linear stability and experiments. *Journal of Fluid Mechanics* 69, 705-719.
- Nakabayashi, K. (1978). Frictional moment of flow between two concentric spheres, one of which rotates. *Journal of Fluids Engineering* 100, 97-106.
- Nakabayashi, K. (1983). Transition of Taylor-Gortler vortex flow in spherical Couette flow. *Journal of Fluid Mechanics* 132, 209-230
- Nakabayashi, K, and W. Sha (2000). Vortical structures and velocity fluctuations of spiral and wavy vortices in the spherical Couette Flow. *Springer-Verlag Berlin Heidelberg LNP* 549, 234-255.
- Nakabayashi, K., W. Sha, and Y. Tsuchida (2005). Relaminarization phenomena and external-disturbance effects in spherical Couette Flow. *Journal of Fluid Mechanics* 534, 327-350.
- Noui-Mehidi, M. N., N. Ohmurab, and K. Kataokab (2005). Dynamics of the helical flow between rotating conical cylinders. *The Journal of Fluids and Structures* 20, 331-344.
- Sobolik, V., T. Jirout, J. Havlica, and M. Kristiawan (2011). Wall shear rates in Taylor vortex flow. *Journal of Applied Fluid Mechanics* 4(2), 25-31.
- Walton, I. C. (1978). The linear stability of the flow in a narrow spherical annulus. *Journal of Fluid Mechanics* 86, 673-693.
- Wimmer, M. (1976). Experiments on a viscous fluid flow between rotating spheres. *Journal of Fluid Mechanics* 79, 317-335.

- Wimmer, M. (1981). Experiments on the stability of viscous flow between two concentric rotating spheres. *Journal of Fluid Mechanics* 103, 117-131.
- Wimmer, M. (1981). Experiments on a viscous fluid between concentric rotating spheres. *Journal of Fluid Mechanics* 78, 317-335.
- Wimmer, M. (1995). An experimental investigation of Taylor vortex flow between conical cylinders. *Journal of Fluid Mechanics* 292, 205-227.
- Yang, R. J. (1996). A numerical procedure for predicting multiple solutions of a spherical Taylor-Couette flow. *International Journal for Numerical Methods in Fluids* 22, 1135-1147.
- Yavorskaya, I. M., Yu. N. Belyaev., A. A. Monakhov (1975). Experimental study of a spherical Couette flow. *Doklady Physics*. 20(4), 256-258.
- Yavorskaya, I. M., Y. N. Belyaev, A. A. Monakhov., N. M. Astaf'eva., S. A. Scherbakov, and N. D. Vvdenskaya (1980, August). Stability, nonuniqueness and transition to turbulence in the flow between two rotating spheres. In: *Theor Appl Mech. Proceedings 15th International Conference*, Toronto, Canada. 17-23, 431-443.
- Yuan, L. (2012). Numerical investigation of wavy and spiral Taylor-Gortler vortices in medium spherical gaps. *Physics of Fluids* 24, 124104.